Powder Technology

Handling and Operations, Process Instrumentation, and Working Hazards

edited by
Hiroaki Masuda
Ko Higashitani
Hideto Yoshida

CRC Press
Taylor & Francis Group

Powder Technology

Handling and Operations, Process Instrumentation, and Working Hazards

Powder Technology

Handling and Operations, Process Instrumentation, and Working Hazards

edited by

Hiroaki Masuda
Ko Higashitani
Hideto Yoshida

CRC Press
Taylor & Francis Group
Boca Raton London New York

CRC Press is an imprint of the
Taylor & Francis Group, an informa business

This material was previously published in *Powder Technology Handbook, Third Edition*. © CRC Press LLC, 2006.

CRC Press
Taylor & Francis Group
6000 Broken Sound Parkway NW, Suite 300
Boca Raton, FL 33487-2742

Printed in the United States of America on acid-free paper
10 9 8 7 6 5 4 3 2 1

International Standard Book Number-10: 1-4200-4412-5 (Hardcover)
International Standard Book Number-13: 978-1-4200-4412-6 (Hardcover)

Library of Congress Cataloging-in-Publication Data

Powder technology: Handling and operations, process instrumentation, and working hazards / [edited by] Hiroaki Masuda and Ko Higashitani.
p. cm.
Includes bibliographical references and index.
ISBN 1-4200-4412-5 (acid-free paper)
1. Masuda, Hiroaki, 1943- II. Higashitani, Ko, 1944-

TP156.P3P645 2006
620'.43--dc22 2006050485

Visit the Taylor & Francis Web site at
http://www.taylorandfrancis.com

and the CRC Press Web site at
http://www.crcpress.com

Preface

Particulate, or powder, technology is a fundamental engineering field that deals with a variety of particles, from submicroscale grains and aggregates to multi-phase colloids.

The applications of powders and particles are rapidly expanding into more diverse technologies, from the information market—including mobile phones, copy machines, and electronic displays—to pharmaceuticals, biology, cosmetics, food and agricultural science, chemicals, metallurgy, mining, mechanical engineering, and many other fundamental engineering fields. Fueling some of the latest developments, nanoparticles are the focus of promising research leading to more effective applications of various particles and powders.

Drawing from the recently published third edition of the acclaimed *Powder Technology Handbook*, this book concentrates its coverage on powder/particle handling methods and unit operations. This independent volume examines the purpose and considerations involved in different processes—including planning, equipment, measurements, and modeling techniques. It focuses on integrated strategies for finding the optimal solutions to problems in any context.

Substantially revised, updated, and expanded, this volume highlights new information on combustion and heating, electrostatic powder coating, and simulation. It also reflects recent data on the health effects caused by the inhalation of fine particles, along with ways to minimize harmful exposure.

While the book consolidates some sections from the last edition for ease of use, it also incorporates the innovative work and vision of new, young authors to present a broader and fully up-to-date representation of the technologies.

We hope this volume will serve as a strong guide for understanding the key aspects of industrial processing for particles and powders and encourage readers to apply the knowledge in this book to real applications, particularly those involving novel particles.

Special acknowledgment is given to all contributors and also to all the original authors whose valuable work is cited in this handbook. We would also like to acknowledge Dr. Matsusaka of Kyoto University, for his collaboration and editing, and we are grateful to our editorial staff at Taylor & Francis Books for their careful editing and production work.

Hiroaki Masuda

Ko Higashitani

Hideto Yoshida

Editors

Hiroaki Masuda is a professor in the Department of Chemical Engineering at Kyoto University, Japan. He is a member of the Society of Chemical Engineers, Japan and the Institute of Electrostatics (Japan), among other organizations, and is the president of the Society of Powder Technology, Japan. His research interests include electrostatic characterization, adhesion and reentrainment, dry dispersion of powder, and fine particle classification. Dr. Masuda received his Ph.D. degree (1973) in chemical engineering from Kyoto University, Japan.

Ko Higashitani graduated from the Department of Chemical Engineering, Kyoto University, Japan in 1968. He worked on hole pressure errors of viscoelastic fluids as a Ph.D. student under the supervision of Professor A. S. Lodge in the Department of Chemical Engineering, University of Wisconsin–Madison, USA. After he received his Ph.D. degree in 1973, he moved to the Department of Applied Chemistry, Kyushu Institute of Technology, Japan, as an assistant professor, and then became a full professor in 1983. He joined the Department of Chemical Engineering, Kyoto University, in 1992. His major research interests now are the kinetic stability of colloidal particles in solutions, such as coagulation, breakup, adhesion, detachment of particles in fluids, and slurry kinetics. In particular, he is interested in measurements of particle surfaces in solution by the atomic force microscope and how the surface microstructure is correlated with interaction forces between particles and macroscopic behavior of particles and suspensions.

Hideto Yoshida is a professor in the Department of Chemical Engineering at Hiroshima University, Japan. He is a member of the Society of Chemical Engineers, Japan and the Society of Powder Technology, Japan. His research interests include fine particle classification by use of high-performance dry and wet cyclones, standard reference particles, particle size measurement by the automatic-type sedimentation balance method, and the recycling process of fly-ash particles. Dr. Yoshida received his Ph.D. degree (1979) in chemical engineering from Kyoto University, Japan.

Contributors

Charles S. Campbell
School of Engineering, Aerospace and Mechanical Engineering
University of Southern California
Los Angeles, California, USA

Toyohisa Fujita
Department of Geosystem Engineering
Graduate School of Engineering
University of Tokyo
Tokyo, Japan

Kuniaki Gotoh
Department of Applied Chemistry
Okayama University
Okayama, Japan

Jusuke Hidaka
Department of Chemical Engineering and Materials Science
Faculty of Engineering
Doshisha University
Kyotanabe, Kyoto, Japan

Ko Higashitani
Department of Chemical Engineering
Kyoto University
Katsura, Kyoto, Japan

Hajime Hori
Department of Environmental Health Engineering
University of Occupational and Environmental Health
Kitakyushu, Fukuoka, Japan

Kengo Ichiki
Department of Mechanical Engineering
The Johns Hopkins University
Baltimore, Maryland, USA

Hironobu Imakoma
Department of Chemical Science and Engineering
Kobe University, Nada-ku
Kobe, Japan

Eiji Iritani
Department of Chemical Engineering
Nagoya University
Nagoya, Chikusa-ku, Japan

Chikao Kanaoka
Ishikawa National College of Technology
Tsubata, Ishikawa, Japan

Yoichi Kanda
Department of Chemical Engineering
Kyoto University
Katsura, Kyoto, Japan

Yoshiteru Kanda
Department of Chemistry and Chemical Engineering
Yamagata University
Yonezawa, Yamagata, Japan

Hisao Makino
Central Research Institute of Electric Power Industry
Yokosuka, Kanagawa, Japan

Hiroaki Masuda
Department of Chemical Engineering
Kyoto University
Katsura, Kyoto, Japan

Shuji Matsusaka
Department of Chemical Engineering
Kyoto University
Katsura, Kyoto, Japan

Kei Miyanami
Department of Chemical Engineering
Osaka Prefecture University
Sakai, Osaka, Japan

Makio Naito
Joining and Welding Research Institute
Osaka University
Ibaraki, Osaka, Japan

Morio Okazaki
Department of Chemical Engineering
Kyoto University
Kyoto, Japan

Jun Oshitani
Department of Applied Chemistry
Okayama University
Okayama, Japan

Isao Sekiguchi
Department of Applied Chemistry
Chuo University
Bunkyo-ku, Tokyo, Japan

Yoshiyuki Shirakawa
Department of Chemical Engineering
and Materials Science
Doshisha University
Kyotanabe, Kyoto, Japan

Minoru Sugita
Ohsaki Research Institute, Inc.
Tokyo, Japan

Minoru Takahashi
Ceramics Research Laboratory
Nagoya Institute of Technology
Tajimi, Aichi, Japan

Isamu Tanaka
Department of Environmental Health
Engineering
University of Occupational and Environmental
Health
Kitakyushu, Fukuoka, Japan

Tatsuo Tanaka
Hokkaido University West
Sapporo, Japan

Toshitsugu Tanaka
Department of Mechanical Engineering
Osaka University
Suita, Osaka, Japan

Ken-ichiro Tanoue
Yamaguchi University
Ube, Yamaguchi, Japan

Yuji Tomita
Department of Mechanical and Control
Engineering
Kyushu Institute of Technology
Kitakyushu, Fukuoka, Japan

Shigeki Toyama
Nagoya University
Nagoya, Japan

JunIchiro Tsubaki
Department of Molecular Design and
Engineering
Nagoya University
Nagoya, Japan

Hirofumi Tsuji
Yokosuka Research Laboratory
Central Research Institute of Electric
Power Industry
Yokosuka, Kanagawa, Japan

Yutaka Tsuji
Department of Mechanical Engineering
Osaka University
Suita, Osaka, Japan

Hiromoto Usui
Department of Chemical Science and Engineering
Kobe University, Nada-ku
Kobe, Japan

Satoru Watano
Department of Chemical Engineering
Osaka Prefecture University
Sakai, Osaka, Japan

Richard A. Williams
Institute of Particle Science and Engineering
School of Process, Environmental, and
Materials Engineering
University of Leeds
West Yorkshire, United Kingdom

Hiroshi Yamato
Department of Environmental
Health Engineering
University of Occupational
and Environmental Health
Kitakyushu, Fukuoka, Japan

Hideto Yoshida
Department of Chemical Engineering
Hiroshima University
Higashi-Hiroshima, Japan

Hiroki Yotsumoto
National Institute of Advanced Industrial
Science and Technology
Tsukuba, Ibaraki, Japan

Shinichi Yuu
Ootake R. & D. Consultant Office
Fukuoka, Japan

Contents

PART I Powder Handling and Operations

Part I

Powder Handling and Operations

1.1 Crushing and Grinding

Tatsuo Tanaka
Hokkaido University West, Sapporo, Japan

Yoshiteru Kanda
Yamagata University, Yonezawa, Yamagata, Japan

1.1.1 INTRODUCTION

Comminution is the oldest mechanical unit operation for size reduction of solid materials and an important step in many processes where raw materials are converted into intermediate or final products. The purposes of comminution are to reduce the size, to increase the surface area, and to free the useful materials from their matrices, and recently it has been involved in modification of the surface of solids, preparation of the composite materials, and recycling of useful components from industrial wastes. Comminution has a long history, but it is still difficult to control particle size and its distribution. Hence, fundamental analysis and optimum operation have been investigated.

A demand for fine or ultrafine particles is increasing in many kinds of industries. The energy efficiency of comminution is very low, and the energy required for comminution increases with a decrease in feed or produced particle size. Research and development to find energy-saving comminution processes have been performed.

1.1.2 COMMINUTION ENERGY

In design, operation, and control of comminution processes, it is necessary to correctly evaluate the comminution energy of solids. In general, the comminution energy (i.e., the size reduction energy) is expressed by a function of a particle size.[1]

Laws of Comminution Energy

Rittinger's Law

Rittinger assumes that the energy consumed is proportional to the produced fresh surface. Because the specific surface area is inversely proportional to the particle size, the specific comminution energy E/M is given by Equation 1.1:

$$\frac{E}{M} = C_R \left(S_p - S_f \right) = C'_R \left(x_p^{-1} - x_f^{-1} \right) \tag{1.1}$$

where S_p and S_f are the specific surface areas of product and feed, respectively, x_p and x_f are the corresponding particle sizes, and C_R and C'_R are constants which depend on the characteristics of materials.

Kick's Law

Kick's law assumes that the energy required for comminution is related only to the ratio of the size of the feed particle to the product particle:

$$\frac{E}{M} = C_k \ln\left(\frac{x_f}{x_p}\right) = C'_k \ln\left(\frac{S_p}{S_f}\right) \tag{1.2}$$

where C_K and C'_K are constants.

Equation 1.2 can be derived by assuming that the strength is independent of the particle size, the energy for size reduction is proportional to the volume of particle, and the ratio of size reduction is constant at each stage of size reduction.

Bond's Law[2]

Bond suggests that any comminution process can be considered to be an intermediate stage in the breakdown of a particle of infinite size to an infinite number of particles of zero size. Bond's theory states that the total work useful in breakage is inversely proportional to the square root of the size of the product particles, directly proportional to the length of the crack tips, and directly proportional to the square root of the formed surface:

$$W = W_i\left(\frac{10}{\sqrt{P}} - \frac{10}{\sqrt{F}}\right) = C'_B\left(S_p^{1/2} - S_f^{1/2}\right) \tag{1.3}$$

where $W(kWh/t)$ is the work input and F and P are the particle size in microns at which 80% of the corresponding feed and product passes through the sieve. $W_i(kWh/t)$ is generally called Bond's work index. The work index is an important factor in designing comminution processes and has been widely used.

Holmes's Law[3]

Holmes proposes a modification to Bond's law, substituting an exponent r, in place of 0.5 in Equation 1.3 as follows:

$$W = W_i\left(\frac{10}{P^r} - \frac{10}{F^r}\right) \tag{1.4}$$

Values of r which Holmes determined for materials are tabulated in Table 1.1.[4]

1.1.3 CRUSHING OF SINGLE PARTICLES

In principle, the mechanism of size reduction of solids is based on the fracture of a single particle and its accumulation during comminuting operations.

Fracture Properties of Solids

In a system composed of an elastic sphere gripped by a pair of rigid parallel platens, the load-deformation curve can be predicted by the theories of Hertz as summarized by Timoshenko and Goodier.[5] The

TABLE 1.1 Values of *r* Determined by Holmes

Materials	Holmes Exponent (*r*)
Amygdaloid	0.25
Malartic	0.40
Springs	0.53
Sandstone	0.66
Morenci	0.73
East Malartic	0.42
Chino Nevada Consolidated	0.65
Real del Monte	0.57
La Luz	0.34
Kelowna Exploratory	0.39
Utah Copper	0.50

elastic strain energy, E (J), input to a sphere up to the instant of fracture is given by the integral of the load acting through the deformation:

$$E = 0.832\left(\frac{1-v^2}{Y}\right)^{2/3} x^{-1/3} p^{5/3} \tag{1.5}$$

where Y (Pa) is Yougth's modulus, v (-), Poisson's ratio, x (m) the diameter of the sphere (particle size), and P (N) is the fracture load. In this system, the compression strength of the sphere, S, is given by Hiramatsu et al.,[6] and the specific fracture energy E/M (J/kg) is given by

$$\frac{E}{M} = C_1 \rho^{-1} \pi^{2/3} \left(\frac{1-v^2}{Y}\right)^{2/3} S^{5/3} \tag{1.6}$$

where p (kg/m^3) is density.

The relationship between the specific fracture energy and the strength for quartz and marble is shown in Figure 1.1.[7]

On the other hand, when two spherical particles, 1 and 2, collide with each other, the maximum stress, S_{max}, generated inside the particles is expressed by a function of particle size, x, relative velocity, v (m/s), and mechanical properties[8]:

$$S_{\max} = C_2 \left(\frac{m_1 m_2}{m_1 + m_2}\right)^{1/5} \upsilon^{2/5} \left(\frac{2}{x_1} + \frac{2}{x_2}\right)^{3/5} \left(\frac{1-v_1^2}{Y_1} + \frac{1-v_2^2}{Y_2}\right)^{-4/5} \tag{1.7}$$

where m_1 (kg) and m_2 are the mass of the particles, and C_2 is a constant. The subscripts 1 and 2 denote two particles.

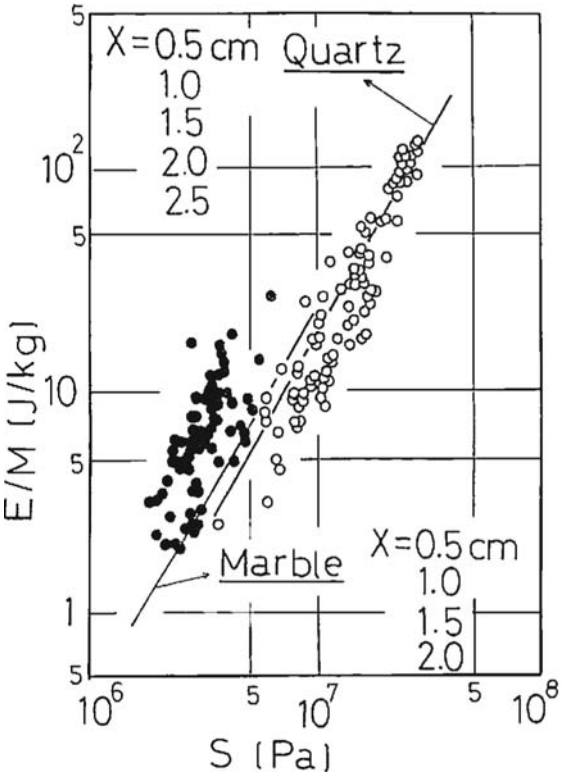

FIGURE 1.1 Relationship between strength S and specific fracture energy E/M.

Variation of Fracture Energy with Particle Size

Strength is a structure-sensitive property and changes with specimen volume. From a statistical consideration of the distribution of the presence of minute flaws,[9] Weibull[10] and Epstein[11] showed that the mean strength of the specimen, S, is proportional to the (–1/m) power of the specimen volume, V (m^3):

$$S = \left(S_0 V_0^{1/m}\right) V^{-1/m} \tag{1.8}$$

where S_0 (Pa) is the strength of unit volume V_0 (m^3), and m is Weibull's coefficient of uniformity. Experimental data lines determined by the least squares method for bolosilicate glass and quartz are shown in Figure 1.2[12] From Equation 1.6 and Equation 1.8, the relationship between specific fracture energy or fracture energy of a single particle, E, and particle size x is obtained as fallows:

$$\frac{E}{M} = C_3 (6)^{5/3m} \rho^{-1} \pi^{(2m-5)/3m} \left(\frac{1-\nu^2}{Y}\right)^{2/3} \left(S_o V_o^{1/m}\right)^{5/3} x^{-5/m} \tag{1.9}$$

$$E = C_4 (6)^{5/3m} \pi^{(5m-5)/3m} \left(\frac{1-\nu^2}{Y}\right)^{2/3} \left(S_o V_o^{1/m}\right)^{5/3} x^{(3m-5)/m} \tag{1.10}$$

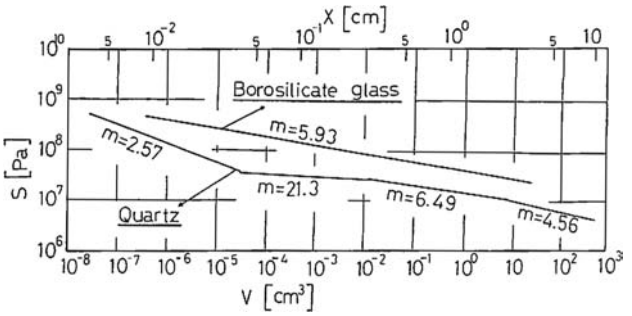

FIGURE 1.2 Variation of strength S with volume V of specimen.

The calculated result for quartz is shown in Figure 1.3.[12] It is important to note that the specific fracture energy increases rapidly for smaller particle size (less than approximately 500 μm), namely, the requirement of large amounts of energy in fine or ultrafine grinding can be presumed. The strength and the specific fracture energy increase also with an increase in loading rate.[13]

Crushing Resistance and Grindability

The importance of crushing resistance or grindability of solid materials and energy efficiency of comminuting equipment have been recognized in determining comminution processes in a variety of industries. Grindability is obtained from a strictly defined experiment. The two typical methods are the following.

Hardgrove Grindability Index (JIS M 8861,1993)

The machine to measure the grindability consists of a top-rotating ring with eight balls 1 in. in diameter. A load of 64 φ 0.5 lb is applied on the top-rotating ring. Fifty grams of material sieved between 1.19 and 0.59 mm is ground for the period of 60 revolutions. The Hardgrove grindability index, H.G.I., is defined as

$$\text{H.G.I.} = 13 + 6.93w \tag{1.11}$$

where w (g) is the mass of ground product finer than 75 μm.

Bond's Work Index (JIS M 4002,1976)

Bond's work index W_i, defined in Equation 1.3,[14] is given by.

$$W_i = \frac{1.1 \times 44.5}{P_1^{0.23} G_{b.p}^{0.82} \left(10/\sqrt{P'} - 10/\sqrt{F}\right)} \tag{1.12}$$

where P_1 is the sieve opening in micron for test grindability, G_{bp} (g/rev) is the ball mill grindability, P' is the product size in microns (80% of product finer than size P_1 passes), and F is the feed size in microns (80% of feed passes). A standard ball mill is 12 in. (305 mm) in internal diameter and 12 in. in internal length, charged with 285 balls, as tabulated in Table 1.2. The lowest limit of the total mass of balls is 19.5 kg. The amount of feed material is 700 cm^3 bulk volume, composed of

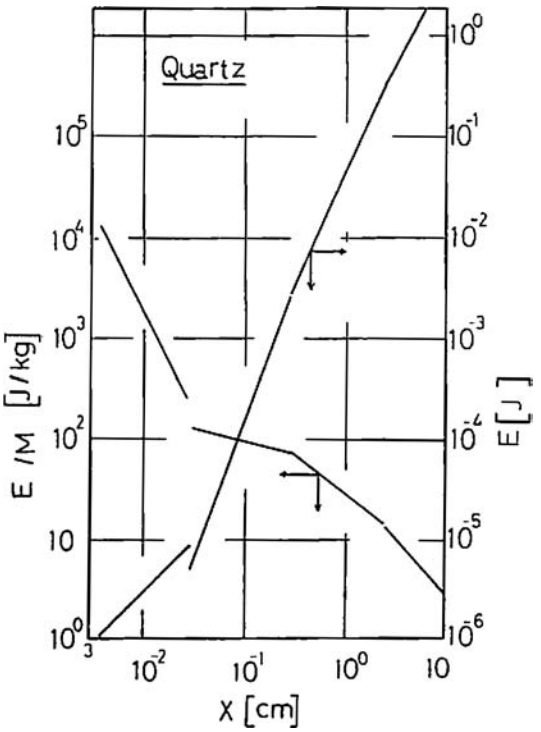

FIGURE 1.3 Relationship between size x and specific fracture energy E/M, or fracture energy E.

TABLE 1.2 Composition of Steel Balls for Measurement by Bond's Work Index

Diameter (mm)	No.of Balls
36.5	43
30.2	67
25.4	10
19.1	71
15.9	94
Sum	285

particles finer than 3360 μm. The mill is rotated a number of times so as to yield a circulating load of 250% at 70 rev/min, where the circulating load is defined as the component ratio of the oversize to the undersize. The process is continued until the net mass of undersize produced per revolution becomes constant $G_{b,p}$ in Equation 1.12. Table 1.3 shows the work index measured by wet process.[15] In fine grinding, when P in Equation 1.3 is smaller than 70 μm, the work index, W_i, is multiplied by a factor f to account for the increased work input. The factor f is found from the following empirical equation[16]:

$$f = \frac{P + 10.3}{1.145P} \left(P \leq 70\mu\text{m}\right) \tag{1.13}$$

TABLE 1.3 Average Work Indexes

Material	Number tested	Average Specific gravity	Work index
All materials tested	1211		14.42
Andesite	6	2.84	18.25
Barite	7	4.50	4.73
Basalt	3	2.91	17.10
Bauxite	4	2.20	8.78
Cement clinker	14	3.15	13.56
Cement raw material	19	2.67	10.51
Coke	7	1.31	15.18
Copper ore	204	3.02	12.73
Diorite	4	2.82	20.90
Dolomite	5	2.74	11.27
Emery	4	3.48	56.70
Feldspar	8	2.59	10.80
Ferro-chrome	9	6.66	7.64
Ferro-manganese	5	6.32	8.30
Ferro-silicon	13	4.41	10.01
Flint	5	2.65	26.16
Fluorspar	5	3.01	8.91
Gabbro	4	2.83	18.45
Glass	4	2.58	12.31
Gneiss	3	2.71	20.13
Gold ore	197	2.81	14.93
Granite	36	2.66	15.05
Graphite	6	1.75	43.56
Gravel	15	2.66	16.06
Gypsumrock	4	2.69	6.73
Iron ore			
Hematite	56	3.55	12.93
Hematite-specular	3	3.28	13.84
Oolitic	6	3.52	11.33
Magnetite	58	3.88	9.97
Taconite	55	3.54	14.60
Lead ore	8	3.45	11.73
Lead-zinc ore	12	3.54	10.57
Limestone	72	2.65	12.54
Manganese ore	12	3.53	12.20
Magnesite	9	3.06	11.13
Molybdenum ore	6	2.70	12.80

(*Continued*)

TABLE 1.3 (Continued) Average Work Indexes

Material	Number tested	Average Specific gravity	Work index
Nickel ore	8	3.28	13.65
Oilshale	9	1.84	15.84
Phosphate rock	17	2.74	9.92
Potash ore	8	2.40	8.05
Pyrite ore	6	4.06	8.93
Pyrrhotite ore	3	4.04	9.57
Quartzite	8	2.68	9.58
Quartz	13	2.65	13.57
Rutile ore	4	2.80	12.68
Shale	9	2.63	15.87
Silica sand	5	2.67	14.10
Silicon carbide	3	2.75	25.87
Slag	12	2.83	9.39
Slate	2	2.57	14.30
Sodium silicate	3	2.10	13.50
Spodumene ore	3	2.79	10.37
Syenite	3	2.73	13.13
Tin ore	8	3.95	10.90
Titanium ore	14	4.01	12.33
Trap rock	17	2.87	19.32
Zinc ore	12	3.64	11.56

Bond[16] proposed a relationship between the work index, W_i, and the Hardgrove grindability index (H.G.I.):

$$W_i = \frac{435}{(\text{H.G.I.})^{0.91}} \tag{1.14}$$

Grindability in Fine Grinding

When the particle sizes of the products are submicron or micronized particles, it will be difficult to estimate the comminution energy by Equation 1.3, Equation 1.12, and Equation 1.13.

Bond[2] had proposed Equation 1.15 for measurement of W_i before Equation 1.12.

$$W_i = 1.1 \times 16 \left(\frac{P_1}{100} \right)^{0.5} \cdot G_{b,p}{}^{-0.82} \tag{1.15}$$

Equation 1.15 is simpler than Equation 1.12. There was not a great difference[17] between W_i calculated by Equation 1.12 and W_i calculated by Equation 1.15. Figure 1.4 shows the relationship

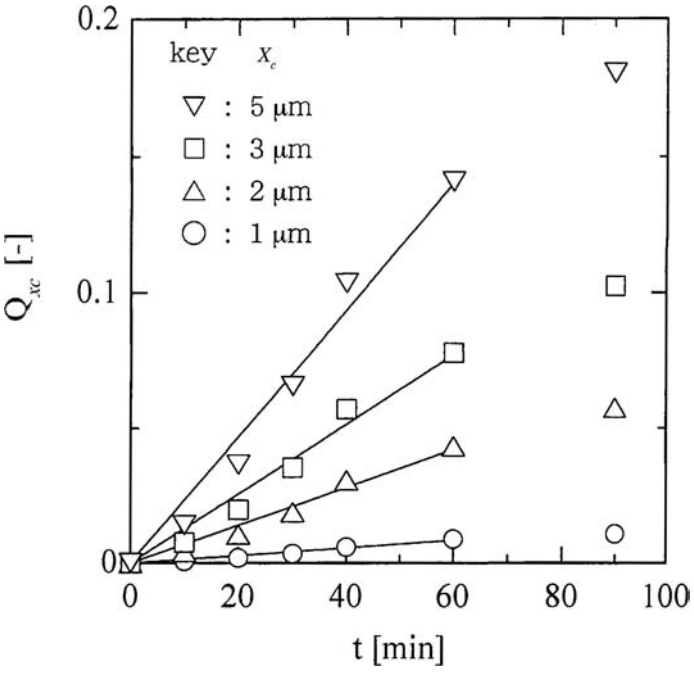

FIGURE 1.4 Relationship between grinding time t and mass fraction finer than size x_c, Q_{xc}.

between the mass fraction Q_{x_c}(–) finer than the particle size (μm) and grinding time (min) in a ball mill grinding of silica glass.[18] In the early stage of grinding, a zero-order increasing rate is applicable, as shown in following equations.

$$Q_{x_c} = k_{x_c} t \tag{1.16}$$

$$W_{x_c} = Q_{x_c} \cdot W_s = k_{x_c} \cdot W_s \cdot t \tag{1.17}$$

where $W_{x\cdot c}$ is the mass of product finer than a size x_c, and W_s is the mass of the feed. From Equation 1.15 through Equation 1.17, the following equations can be obtained:

$$W_i \propto P_1^{0.5} \cdot G_{b_p}^{-0.82} \propto x_c^{0.5} \cdot \left(k_{x_c} \cdot W_s\right)^{-0.82} \tag{1.18}$$

$$W_{i_c} = x_c^{0.5} \cdot \left(k_{x_c} \cdot W_s\right)^{-0.82} \tag{1.19}$$

where W_{x_c} is proportional to W_i, which was proposed by Bond. W_{i_c} could be estimated by the examination of the zero-order increasing rate constant of the mass fraction less than a sieving size using an arbitrary ball mill.

Figure 1.5 shows the relationship between sieving size, x_c, and W_{i_c} for silica glass.[18] It was presumed that the work index could be approximately constant to a sieving size of 20 μm and increased in the range of a size less than 20 μm. It was also found that large amounts of energy are necessary to produce fine or ultrafine particles.

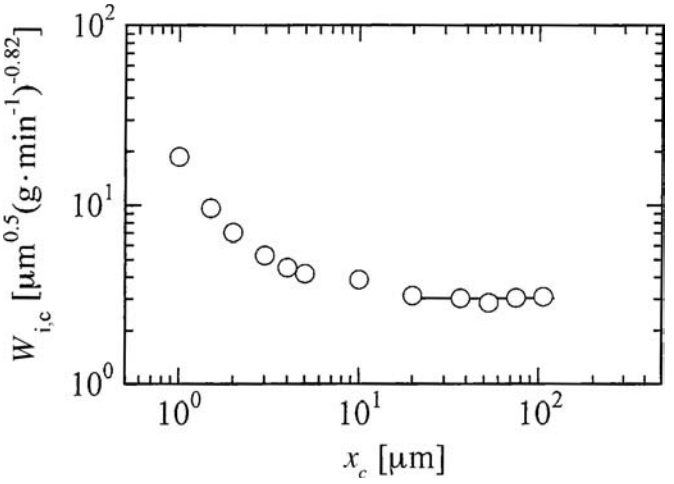

FIGURE 1.5 Relationship between sieving size x_c and corresponding work index W_{I_c}.

1.1.4 KINETICS OF COMMINUTION

A pulverizing machine is to be designed and operated by pursuing the comminution process of particle assemblage with the elapsed time. The size distribution after fracture of a single particle is derived by applying a stochastic theory by Gilvarry,[19] Gaudin and Meloy,[20] or Broadbent and Callcot.[21] These theories are based on the idea that some microcracks preexisting in the solid body are activated with stress and absorb elastic strain energy, so that the cracks develop rapidly and collide with each other to yield fragments of distributed sizes. The undersize cumulative fraction $B(\gamma, x)$ produced from a single particle of size γ is called a breakage function and is written as follows:

Gilvarry:

$$B(\gamma,x) = 1 - \exp\left[-\left(\frac{x}{c_1}\right) - \left(\frac{x}{c_2}\right)^2 - \left(\frac{x}{c_3}\right)^3\right] \tag{1.20}$$

Gaudin and Meloy:

$$B(\gamma,x) = 1 - \left[1 - \left(\frac{x}{\gamma}\right)\right]^j \tag{1.21}$$

Broadbent and Callcot:

$$B(\gamma,x) = \frac{1 - \exp(-x/\gamma)}{1 - \exp(-1)} \tag{1.22}$$

where x is the particle size, c_1, c_2, and c_3 are constants, and j is the number of fragments or 10. They may be approximated as

$$B(\gamma,x) = \left(\frac{x}{\gamma}\right)^m \tag{1.23}$$

where m is a constant.[22] The derivative $\partial B/\partial x$ is called a distribution function appearing later.

With respect to the mass–size balance in batch grinding, the mass increment of a component of size x during a differential time interval dt is expressed by removal of a portion of the component due to selective grinding and by production of the same component due to selectively grinding a portion of all the coarser particles followed by the distribution to the noted size range, as illustrated in Figure 1.6:

$$\frac{\partial^2 D(x,t)}{\partial t\ \partial x} = -\frac{\partial D(x,t)}{\partial x} S(x,t) + \int_x^{x_m} \frac{\partial D(\gamma,t)}{\partial \gamma} S(\gamma,t) \frac{\partial B(\gamma,x)}{\partial x} dy \tag{1.24}$$

where $S(\gamma,t)$ is the probability density for particles of size γ to be selected for grinding and it is called a selection function or rate function, t is the grinding time, and X_m is the maximum size present. Thus, the rate of comminution of particle assemblage is determined by the size distribution after crushing a single particle and by the probability that each particle is selected for crushing within a certain time. Assuming Equation 1.23 for $B(\gamma,x)$ and the empirical relationship

$$S(x,t) = Kx^n \tag{1.25}$$

for $S(x,t)$ (Bowdish, 1960), the oversize cumulative fraction, $R(x,t) = 1 - D(x,t)$, is obtained by integration of Equation 1.24 using a rate constant, K:

$$m = n:$$

$$R(x,t) = R(x,0)\exp -Kx^n t \tag{1.26}$$

$$m \neq n:$$

$$R(x,t) \approx R(x,0)\exp[-(\mu K x^n t)^v] \tag{1.27}$$

where $R(x,0)$ is the initial size distribution and can be regarded as unity if the grinding time t is long enough. μ and v are determined only by the value of m/n, as indicated in Figure 1.7. The size distribution is found to vary with grinding time in the Rosin–Rammler type, which was first confirmed experimentally by Chujo[23] using a ball mill. The selection function or the rate constant has been experimentally determined by Shoji and Austin[24] for ball milling, as shown in Figure 1.6, in which

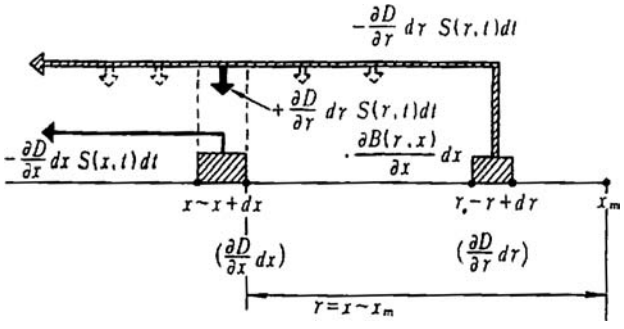

FIGURE 1.6 Explanation of mass balance in comminution process. [From Austin, L.G., and Klimpel, R.R., Ind. Eng. Chem., 56, no. 11, 18–29, 1964.]

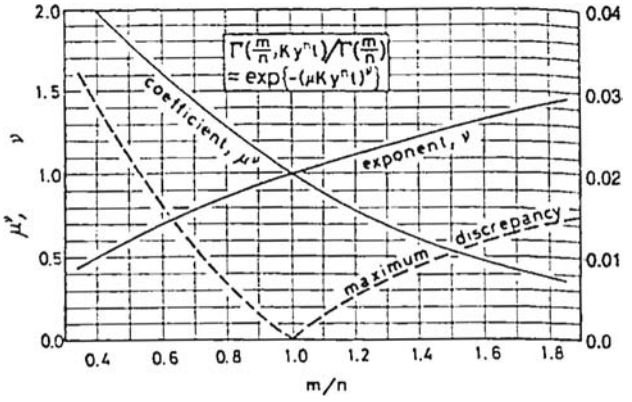

FIGURE 1.7 Approximation of Equation 1.25 by exponential function.

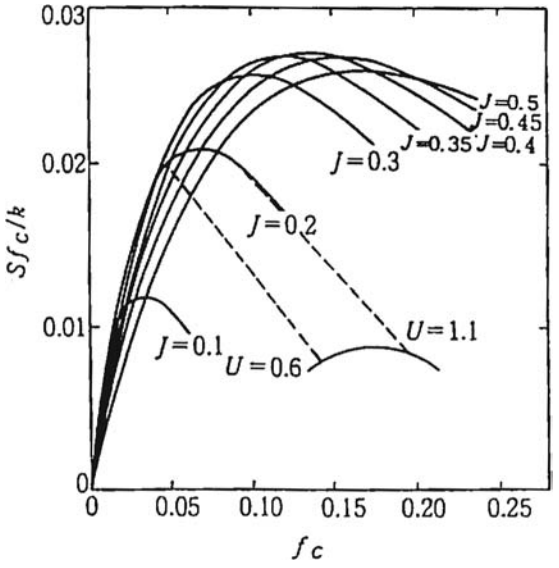

FIGURE 1.8 Variation of relative absolute rate of breakage with powder and ball filling for dry grinding.

$S(x)$ is depicted in relation to f_c, the fractional holdup of particles in a mill, to J, the ball filling degree, and U, the particle filling in the interstice of balls. The grinding rate is reported by Tanaka[25] for ultrafine grinding based on the current experimental works using very small beads in ball, vibration, planetary, and stirred milling, as

$$S(x) \propto \rho\left(\frac{x}{d}\right)\exp\left(-\frac{d_m}{d}\right) \tag{1.28}$$

where d is the beads' diameter, d_m the optimum beads' diameter as a function of the beads density ρ, colliding speed, size, and strength of material crushed.

1.1.5 GRINDING OPERATIONS

To reduce the strength or the toughness of the material crushed, wet process grinding, the addition of grinding aids, and cryogenic grinding are proposed. The additives are likely to reduce the surface energy, leading to facilitating grinding of the particles. In addition to this, newly formed surfaces are active enough for stronger chemical bonding, so that surface modification can be expected by the grinding operation.

Furthermore, to prepare the size distribution required for product quality, a multipass of ground material through a mill and a classifier are necessary, as noted below.

Internal Classification System

The classification mechanism is assembled in a grinding mill. For example, an air-swept mill adopts internal classification by flowing fluids such as air through the mill, where particles finer than a critical size x_c are removed from the machine immediately after grinding. Then the following mass balance holds[26]:

$$F\left(\frac{dR_p(x)}{dx}\right) = H\int_{x_c}^{x_m}\left(\frac{dR(\gamma)}{d\gamma}\right)S(\gamma)\left(\frac{\partial B(\gamma,x)}{\partial x}\right)d\gamma \tag{1.29}$$

where F is the feed to a continuous grinding machine, H is the holdup of particles in the machine, and the subscript p denotes product. Using Equation 1.23 and Equation 1.25 along with the conditions

$$\int_{x_c}^{x_m}\left(\frac{dR(\gamma)}{d\gamma}\right)d\gamma = 1;\ \int_0^{x_c}\left(\frac{dR_p(x)}{dx}\right)dx = 1$$

the ideal size distribution of the ground material is given in the case where Equation 1.30 is applicable and sorting by a clean-cut classification is assumed:

$$\frac{F}{KH} = x_c^n \tag{1.30}$$

$$R_p(x) = 1 - \left(\frac{x}{x_c}\right)^n \tag{1.31}$$

Closed-Circuit Grinding System

In contrast to the preceding system, a closed-circuit system is characterized by an external classifier involved in the system. The ground material, D, is continuously sent to a classifier, where only the fine component is removed as the finished product, P. The coarse material is recirculated to the mill, as shown in Figure 1.9. Increasing the circulating load T, it is possible to avoid overcrushing so as to increase the grinding capacity. Controlling the size distribution of the finished product is also possible to some extent.

In a clean-cut classifier[27], the cumulative oversize fraction or the ground particles, R_D, is obtained from Equation 1.26 for the average residence time t_0 (= H/F) in the mill as

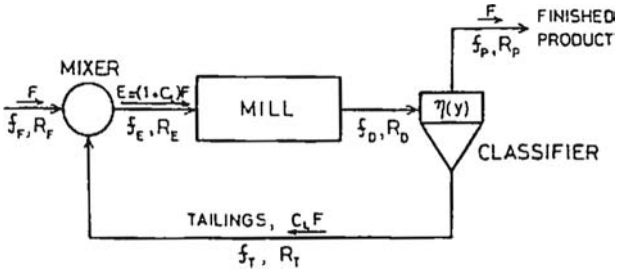

FIGURE 1.9 Typical connection of closed-circuit grinding system.

$$R_D(x) = \exp\left(-\frac{Kt_0 x^n}{1+\mathrm{CL}}\right) \tag{1.32}$$

where the average residence time is given by the overall residence time t_0 ($= H/F$) in this circuit and the circulating ratio CL as

$$i_{\mathrm{av}} = \frac{H}{E} = \frac{H}{F(1-\mathrm{CL})} = \frac{t_0}{1-\mathrm{CL}} \tag{1.33}$$

$$\mathrm{CL} = \frac{T}{P} = \frac{T}{F} = \frac{R_D(x_\mathrm{c})}{1-R_D(x_\mathrm{c})} \tag{1.34}$$

hence, the cutoff size x_c is given by combining Equation 1.32 and Equation 1.34 as

$$Kt_0 x_\mathrm{c}^n = \ln\left[1+\left(\frac{1}{\mathrm{CL}}\right)\right]^{1+\mathrm{CL}} \tag{1.35}$$

The characteristic classification size x_c^* of x_c corresponding to infinite CL is also obtained from Equation 1.34 and Equation 1.35, as

$$x_\mathrm{c}^{*n} = \left(\frac{F}{KH}\right) \tag{1.36}$$

As the clean-cut size distribution of product, $R_\mathrm{p}(x)$, is written by

$$R_\mathrm{p}(x) = \frac{R_D(x) - R_D(x_\mathrm{c})}{1-R_D(x_\mathrm{c})} \tag{1.37}$$

the following are obtained using the equations above:

$$R_p\left(\frac{x}{x_c^*}\right)=(1+\mathrm{CL})\exp\left(-\frac{\left(x/x_c^*\right)^n}{1+\mathrm{CL}}\right)-\mathrm{CL} \tag{1.38}$$

$$\left(\frac{x_c}{x_c^*}\right)^n=(1+\mathrm{CL})\ln\left[1+\left(\frac{1}{\mathrm{CL}}\right)\right] \tag{1.39}$$

The interrelationship between the above two equations is graphed in Figure 1.10. The chart is used such that a desired size ratio (x_{30}/x_{70}) of product at $R_p = 30\%$ and 70%, for example, is fitted to the horizontal distance between the two corresponding curves. Hence, x_c^* is calculated from the value on the abscissa using either x_{30} or x_{70}; then, x_c and CL are read from the ordinate on both sides. The flow system of the closed circuit can be designed by use of CL and F for the transportation equipments and x_c for the classifier. The mill design should be made on basis of H in Equation 1.36 for a known grinding rate constant K as well as F and x_c^*.

In the case of a non-clean-cut classifier,[28] classification performance can be expressed by two parameters, A and S, in a mathematical model of the partial classification efficiency $\eta(x)$ as follows:

$$\eta(x)=\left\{1+\exp\left[\left(\frac{4S}{A}\right)\left[1-\left(\frac{x}{x_c}\right)^A\right]\right]\right\}^{-1} \tag{1.40}$$

where $A = 1.5$ and $S = 1.0$ for air separators, and $A = 1.0$ and $S = 0.5$ for hydrocyclones. Choosing a reference curve in Figure 1.11 to be fitted to the desired cumulative undersize distribution of the finished product, the size corresponding to 1.0 on the abscissa is equal to x_c^* (for $v = 1$ in Equation 1.27), and the cumulative undersize $D_p(1)$ on the ordinate is connected with CL for specific values of S and A in Figure 1.12. Then, the value of CL indicates x_c/x_c in Figure 1.13; thus, the cutoff size, x_c, is obtained from x_c^*. Figure 1.14 illustrates some partial classification efficiency curves modeled by use of the two parameters S and A.[28]

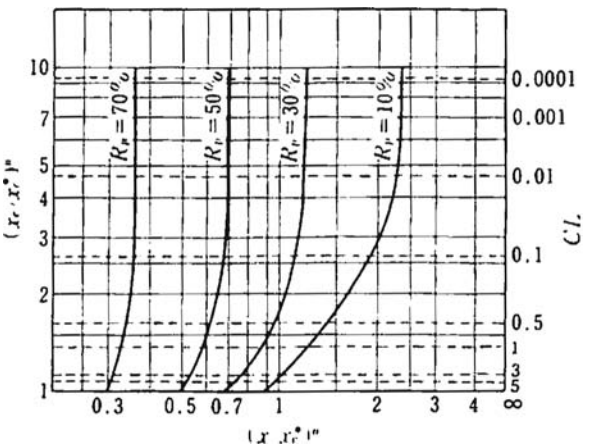

FIGURE 1.10 Collinear chart for ideal classification. [From Furuya, M., Nakajima, Y., and Tanaka, T., *Ind. Eng. Chem. Process. Des. Dev.,* 10, 449–456, 1971.]

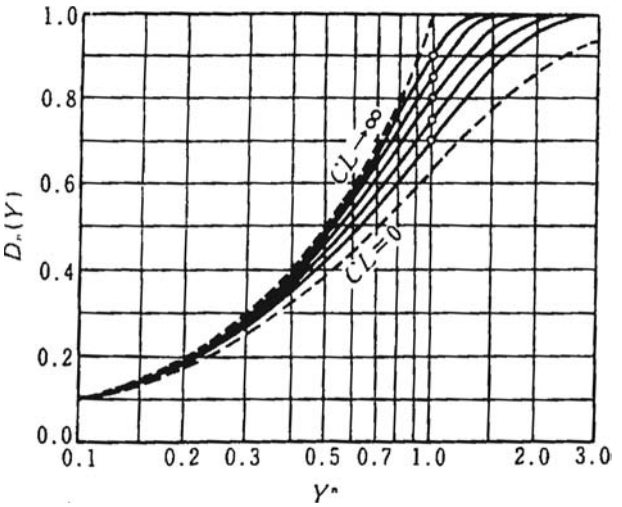

FIGURE 1.11 Reference curve for size distribution of product. (30) [From Furuya, M., Nakajima, Y., and Tanaka, T., *Ind. Eng. Chem. Process. Des. Dev.,* 12, 18–23, 1973.]

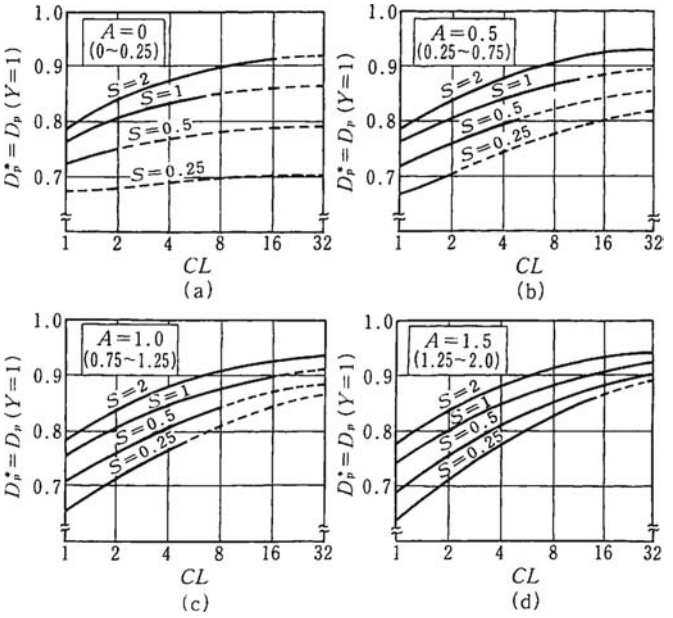

FIGURE 1.12 Relationship among classification parameters, circulating ratio, and undersize fraction of product at $x = x_c^*$. [From Furuya, M., Nakajima, Y., and Tanaka, T., *Ind. Eng. Chem. Process. Des. Dev.,* 12, 18–23, 1973.]

Alteration of the size distribution of the finished product is possible by some combinations of mills and classifiers, as well as feed positions. The analysis is given by Tanaka,[29] taking advantage of Figure 1.10. Grinding capacity increases in general with increasing CL due to the reduction of overcrushed fine particles. In this sense, it is worthwhile noting that when CL in Equation 1.38 tends to infinity, $R_p(x)$ becomes the same as Equation 1.31, the internal classification mechanism.

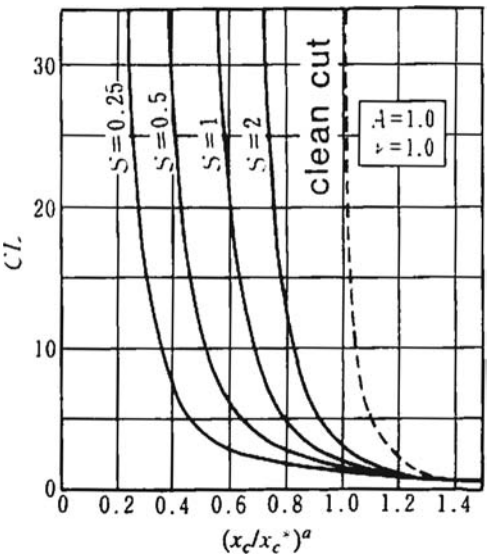

FIGURE 1.13 Relationship among classification parameters, circulating ratio, and $(x_c/x_c^*)^n$.

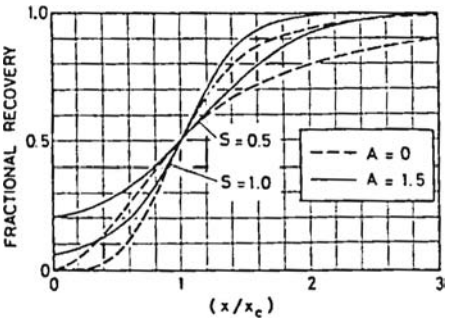

FIGURE 1.14 Fractional recovery curves calculated from the mathematical model (Equation 1.35 and Equation 1.36).

1.1.6 CRUSHING AND GRINDING EQUIPMENT

A major objective of comminution is to liberate minerals for concentration processes. Another objective is to produce particles of a required sizes. Comminution processes generally consist of several stages in series. Various types of crushing and grinding equipments have been used industrially as a mechanical way of producing particulate solids. The working phenomena in these types of equipment are complex, and different principles are adopted in the loading, such as compression, shear, cutting, impact, and friction; in the mechanism of force transmission or the mode of motion of grinding media, such as rotation, reciprocation, vibration, agitation, rolling, and acceleration due to fluids; and in the operational method, such as dry or wet system, batch or continuous operation, association of internal classification or drying and so on. But, in practice, it is most common to classify comminution processes into four stages by the particle size produced. Although the sizes are not clear cut, they are called the primary (first), intermediate (second), fine (third), and ultrafine (fourth) stages, according to the size of ground product. On the basis of the above classification, typical equipment types and their structure and characteristics are mentioned briefly below.

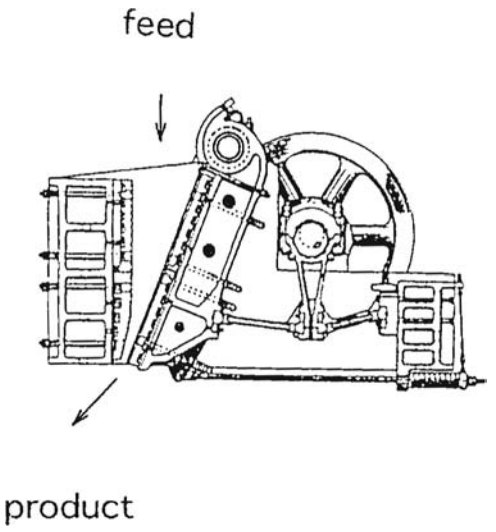

FIGURE 1.15 Jaw crusher.

Crushers

Crushers are widely used as the primary stage to produce particles finer than about 10 cm in size. They are classified as jaw, gyratory, and cone crushers based on compression, cutter mill and shredder based on shear, and hammer crusher based on impact.

Jaw Crusher

The jaw crusher shown in Figure 1.15 consists essentially of two crushing surfaces, inclined to each other. Material is crushed between a fixed and a movable plate by reciprocating pressure until the crushed products become small enough to fall through the narrowest gap between the crushing surfaces.

Gyratory Crusher

The essential features of a gyratory crusher are a solid cone on a revolving shaft, placed within a hollow shell which may have vertical or conical sloping sides, as shown in Figure 1.16. Material is crushed when the crushing surfaces approach each other, and the crushed products fall through the discharging chute.

Hammer Crusher, Swing-Hammer Crusher, and Impactor

These are used either as a one-step primary crusher or as a secondary crusher for products from a primary crusher. Pivoted hammers are mounted on a horizontal shaft, and crushing takes place by the impact between the hammers and breaker plates. A cylindrical grating or screen can be placed beneath the rotor. Materials are reduced to a size small enough pass through the bars of the grating or screen. Hammers are symmetrically designed. The size of product can be regulated by changing the spacing of the grate bars or the opening of the screen, and also by lengthening or shortening the hammer arms.

Intermediate Crushers

Intermediate crushers produce particles finer than about 1 cm. The roller mill, crushing roll, disintegrator, screw mill, edge runner, stamp mill, pin mill, and so on belong to this category. Roll

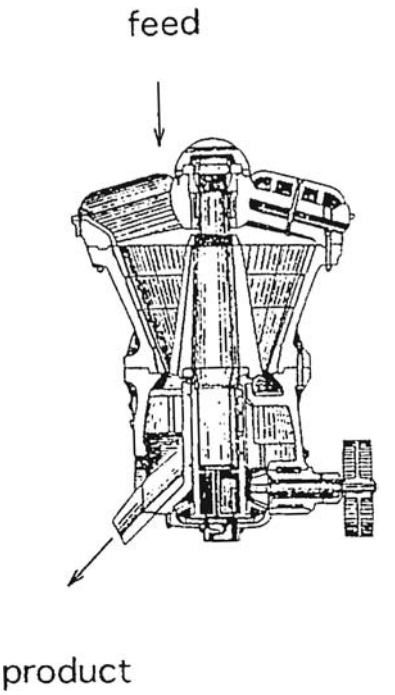

FIGURE 1.16 Gyratory crusher.

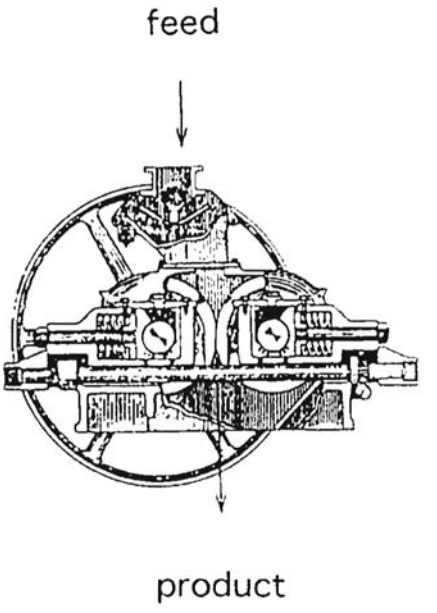

FIGURE 1.17 Crushing roll.

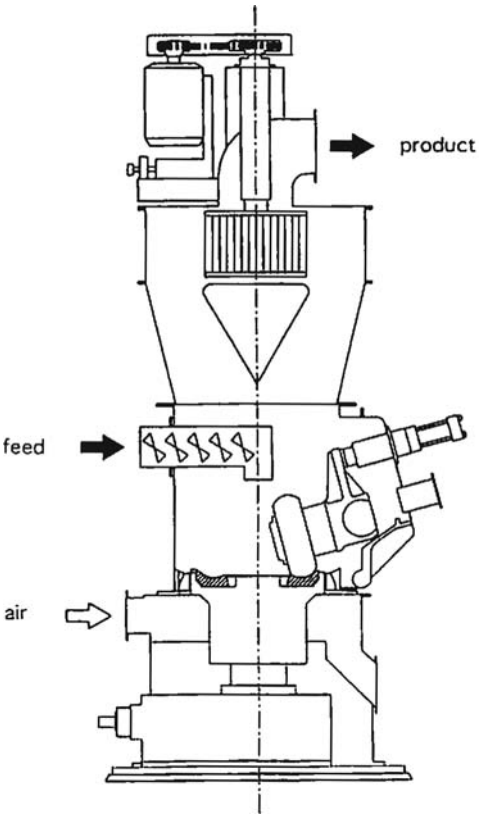

FIGURE 1.18 Roller mill.

crushers are of many types. They consist of at least one cylinder rotating on its principal axis, which nips material with two surfaces to compress and break the material into pieces. Figure 1.17 shows a typical crushing roll. It consists of two cylinders mounted on horizontal shafts, which are driven in opposite directions. The distance between the cylinders (rollers) is usually made adjustable. The size of feed materials is determined by the diameter of the cylinders, the required size of products, and the angle of nip. Recently, high-pressure roller mills (100–200 MPa) are available to comminute finely brittle materials.[30] Figure 1.18 shows a typical roller mill. Roller mills have been actively used for preparation of fine particles. Material is fed to the center of the horizontally rotating table, conveyed to its circumference by centrifugal force, ground by several units of rollers on the concave table, and moved toward the circumference.

Fine-Grinding Equipment

Fine-grinding equipment produces particles finer than about 10 μm. There are many kinds of machines in this category. They are roughly classified into three types: ball-medium type, medium agitating type, and fluid-energy type.

In a ball-medium type, the grinding energy is transferred to materials through media such as balls, rods, and pebbles by moving the mill body. Based on the mode of motion of the mill body, ball-medium mills are classified as tumbling ball mills, vibration mills, and planetary mills.

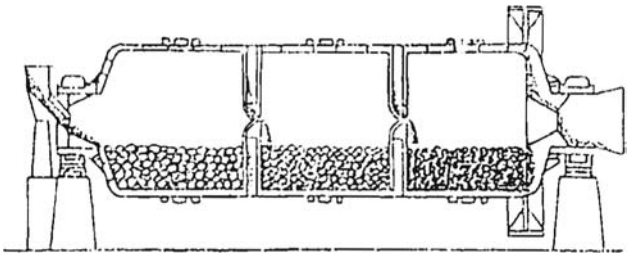

FIGURE 1.19 Compartment mill.

1. A tumbling mill or a ball mill is most widely used in both wet and dry systems, in batch and continuous operations, and on small and large scales. The optimum rotational speed is usually set at 65 to 80% of critical speed, N_c (rpm), when the balls are attached to the wall due to centrifugation:

$$N_c = \frac{42.3}{\sqrt{D_m}} \tag{1.41}$$

where D_m is the mill diameter in meters. It is desirable to reduce the ball size in correspondence with the smaller size of the feed materials, as in a compartment mill, shown in Figure 1.19, and a conical ball mill.

2. A vibration mill is driven by eccentric motors to apply a small but frequent impact or shear to the grinding media. Loose bodies or media contained in a shell cause it to vibrate. In contrast to tumbling mills, the media in vibration mills move only a few millimeters through a complex path, shearing as well as impacting the material between them. The apparent amount of media is 75 to 85% by volume, which is about two times as much as filling mills. One of the advantages of vibration mills compared with tumbling mills is the higher grinding rate in the range of fine particles. But it is unsuitable for heat-sensitive materials.
3. A planetary mill consists of a revolving base disk and rotating mill pots, as shown in Figure 1.20. Materials are ground in a large centrifugal field by the force generated during revolution and rotation. The intensity of acceleration can be increased up to 150g on the scale of gravitational acceleration. It is predicted that the grinding mechanism consists of compressive, abrasive, and shear stresses of the balls. Planetary mills are also used in the study of mechanical alloying and composite particles.[31]

A fluid-energy mill is widely noted as a jet mill. In a jet mill, the materials are ground by the collision of a particle with a particle, a wall, or a plate of the grinding vessel (chamber). The collision energy is generated by a high-speed jet flow. Fluid-energy mills may be classified in terms of the mill action. In one type of mill, the energy is generated by high-velocity streams at a section or whole periphery of a grinding and classification vessel. There are the Micronizer and Jet-O-Mizer shown in Figure 1.21 and others of this type. In Majac and other mills, two streams convey particles at high velocity into a vessel where they impact on each other. A fluid-energy mill has no movable mechanical parts, and it has advantages such as dry and continuous operation without a temperature rise, and controlling the particle size by the feed rate of materials and the velocity of jet stream. But the energy efficiency is low, and the power cost is high.

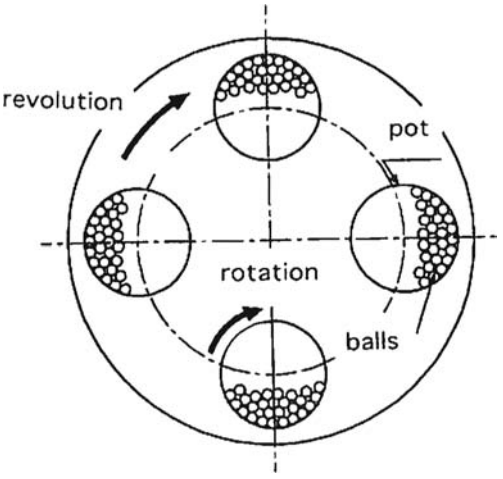

FIGURE 1.20 Planetary mill.

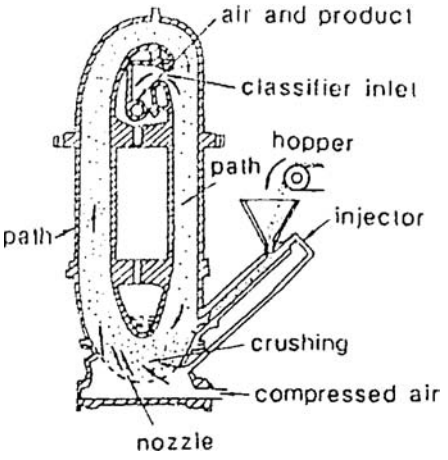

FIGURE 1.21 Jet mill.

Ultrafine Grinding Equipment

Ultrafine grinding equipments produce particles finer than about 1 μm. The medium agitating mills (stirred media mills) are in this category.

A medium agitating mill is regarded as one of the most efficient devices for micronizing materials and has been actively used for preparation of ultrafine particles. In this technique, a large number of small grinding media are agitated by impellers, screws, or disks in a vessel. Breakage occurs mainly by collision of the media. It is classified into three types by agitating mode. Medium agitating mills could produce submicron particles.

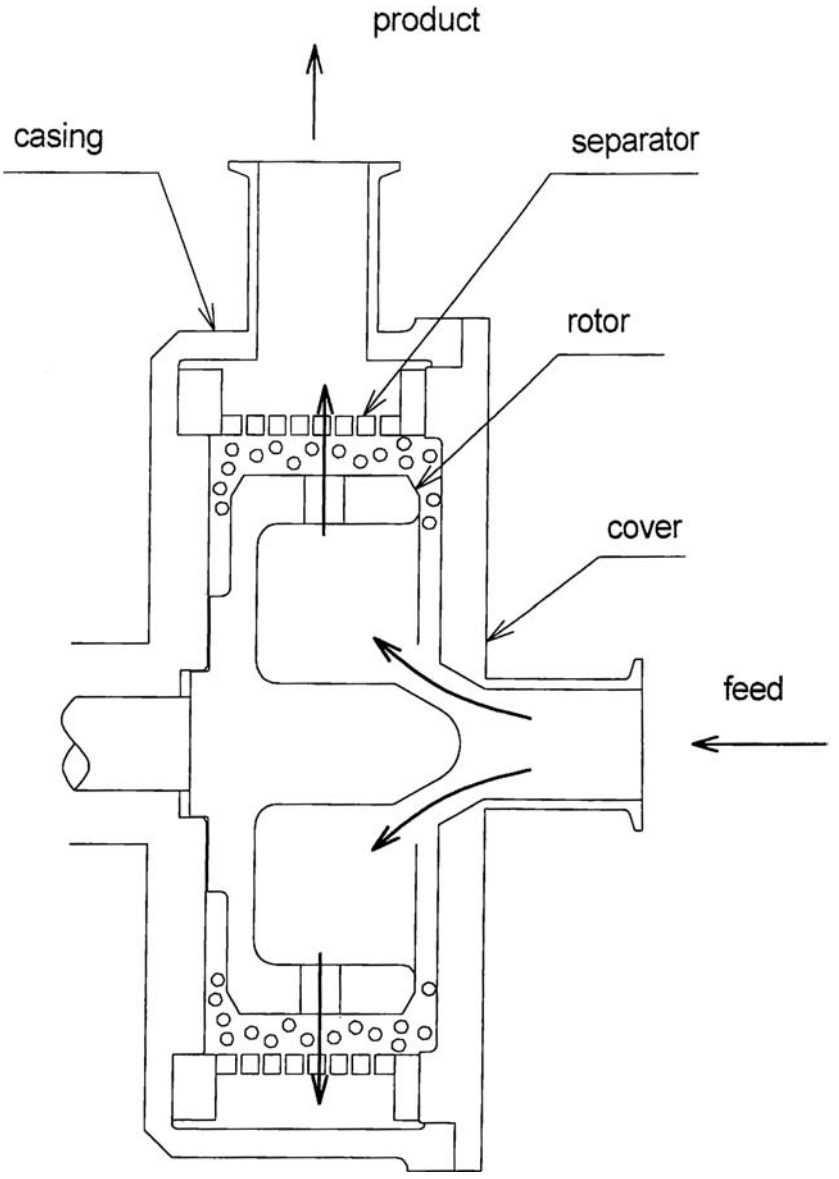

FIGURE 1.22 Stirred mill.